Cooperation Between Grid-Forming Wind Turbine Generators and Primary Frequency Regulation

Meng Chen and Ioannis Lestas
Department of Engineering
University of Cambridge
Cambridge, United Kingdom
mc2545@cam.ac.uk; icl20@cam.ac.uk

Yufei Xi and Lin Cheng
State Key Laboratory of Power System Operation and Control
Tsinghua University
Beijing, China
xyf.2022@tsinghua.org.cn; chenglin@mail.tsinghua.edu.cn

***Abstract*—Conventional grid-forming (GFM) control strategies rarely consider coordination with wind turbine generators (WTGs). This paper proposes a specification-based design scheme that enables WTGs to actively support primary frequency regulation within the allowable frequency deviations by fully using the available power reserves. The proposed strategy prevents the WTG output from moving to the low-speed region when there is a decrease in frequency, which would further reduce system frequency, or to the high-speed region during a frequency, which would exceed allowable power reserves and cause power waste. Simulation results validate the superior performance and effectiveness of the proposed strategy.**

***Index Terms*—Primary frequency control, grid-forming, wind power generator, frequency deviation, power reserve**

I. Introduction

Conventional wind turbine generators (WTGs) typically operate in grid-following (GFL) maximum power point tracking (MPPT) mode, which prevents them from responding to grid disturbances [1]. As WTGs are increasingly integrated into modern power systems, they are expected to participate in primary frequency regulation [2]. This requires new control strategies beyond conventional GFL-MPPT operation.

The key to enabling WTGs in frequency regulation is linking their output power to grid frequency. In GFL mode, it can be achieved by defining a reference trajectory that deviates from MPPT output when a frequency event is detected [3]. Although various trajectory-based strategies have been proposed, they may cause secondary frequency dips, and some key parameters are often determined through trial and error [3]–[5]. Moreover, since the trajectory is predetermined and returns to MPPT operation after each event, such open-loop control lacks flexibility to handle different frequency disturbances and cannot replicate the droop characteristics of primary regulation in synchronous generators (SGs).

Closed-loop methods can formulate power references using grid frequency feedback [6], which can improve dynamic performance [7] and readily incorporate droop characteristics [8]. However, after frequency decreases, a WTG operating in MPPT mode tends to settle at a lower rotor speed after the transient support response [9]. Thus, instead of increasing power to support the grid, the WTG reduces its power, further aggravating the frequency decline. To address this issue, WTGs can be operated in a deloaded mode with a power reserve for primary frequency regulation [10]. Nevertheless, determining the appropriate deloading level requires further investigation to ensure favorable support characteristics.

In contrast to GFL control, GFM control is more suitable for scenarios with high penetration of WTGs. It enables power converters to explicitly emulate the dynamics of conventional SGs [11]. Although various advanced schemes have been proposed to improve dynamic performance, in steady-state operation, most of these methods behave as droop-based primary frequency regulation [12]. However, since they seldom consider coordination with the DC source, when directly applied to WTGs, such approaches may lead to unsatisfactory regulation performance. Similar to GFL control, performance can be improved by setting appropriate power references [13]–[15]. Nevertheless, since existing schemes do not explicitly account for regulation specifications, they may fail to meet those requirements during primary frequency regulation.

This paper proposes a new deloading strategy based on predefined limits on allowable frequency deviation and power reserve limits. As a result, the WTGs can automatically perform frequency regulation within these specifications in response to grid frequency variations. Although the basic idea of deloading operation is not new, the proposed specific design can achieve the cooperation between GFM-WTGs and primary frequency regulation compared to other deloading design.

II. WTGs with GFM Control

A. System Description

Fig. 1 shows a typical configuration of a grid-connected GFM permanent magnet SG (PMSG)-based WTG. To support the grid, the GFM control emulates the frequency and voltage regulation characteristics of an SG as shown in Fig. 2.

The angular frequency ω is determined by

$$2H\dot{\omega} = P_{st} - p - p_{prim} \tag{1}$$

This work was funded by UK Research and Innovation (UKRI) under the UKRI Postdoctoral Fellowship Guarantee Grant [EP/Z001889/1]. Meng Chen would like to acknowledge the Department of Engineering, University of Cambridge, for the support of the Fellowship. Yufei Xi would like to acknowledge the support from the Beijing High-Level Overseas Talent Return Program (no. 04200000125). The contents reflect only the authors' view and not the views of the University or the UKRI.

979-8-3315-8138-1

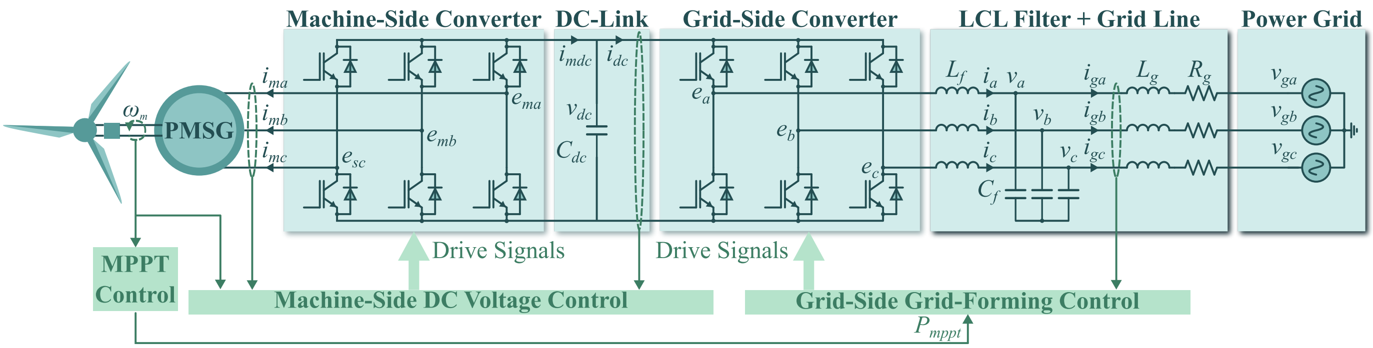

Fig. 1. Configuration of GFM-PMSG-WTG system.

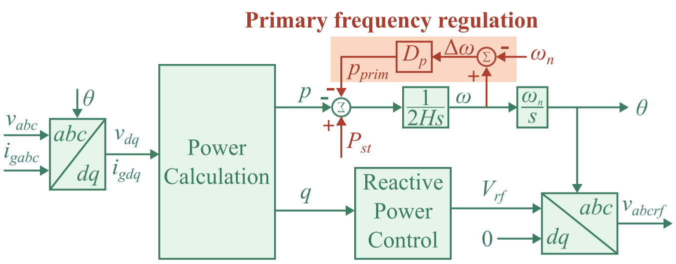

Fig. 2. Control block diagram of grid-side GFM control.

where H is the virtual inertia constant, P_{st} is the set-point active power, and p is the actual active power output. The term p_{prim} represents the power for primary frequency regulation by emulating droop characteristics and is defined as

$$p_{prim} := D_p(\omega - \omega_n) = D_p\Delta\omega \tag{2}$$

where D_p is the droop coefficient and ω_n is the nominal angular frequency. Although only a basic GFM control is considered in Fig. 2, the analysis is generally applicable to advanced schemes with steady-state droop characteristics.

Existing studies on GFM control usually treat P_{st} as a free parameter, which is suitable for applications involving energy storage systems. However, in the case of WTGs, P_{st} is typically defined as a function of the MPPT power P_{mppt}, denoted as

$$P_{st} = f(P_{mppt}) \tag{3}$$

where

$$P_{mppt} = (1/2)\rho\pi R^5 C_{popt}(\lambda_{opt},\ \beta)(\omega_m^3/\lambda_{opt}^3). \tag{4}$$

Here ρ is the air density, R is the turbine blade length, ω_m is the rotor speed, λ is the tip-speed ratio, β is the pitch angle, which is set to 0° in this paper, and C_p is the power coefficient. The subscript "*opt*" denotes the optimal value of the corresponding variable.

Due to (3), the GFM regulation characteristics on the AC side are closely coupled with the characteristics of the WTG. Therefore, potential issues may arise if the GFM-WTG and the primary frequency regulation are not properly coordinated.

B. Problems in Primary Frequency Regulation

Regardless of the specific advanced GFM control used for wind turbines, existing strategies for setting P_{st} generally fall into two categories, i.e., MPPT control and deloading control.

1) Characteristics without Deloaded Operation: When directly applying GFM control to WTGs, P_{st} can be simply set to P_{mppt}, i.e.,

$$P_{st} = P_{mppt}. \tag{5}$$

Combining (1), (2), and (5), the steady-state primary frequency regulation characteristics are given by

$$p_{ss} = P_{mppt} - D_p\Delta\omega_{ss} \tag{6}$$

where $\Delta\omega_{ss}$ is the steady-state frequency deviation resulting from the droop response, and p_{ss} denotes the corresponding steady-state active power output. Meanwhile, the captured wind power P_w is expressed as

$$P_w = (1/2)\rho\pi R^2 C_p(\lambda,\ \beta)v_{wind}^3 \tag{7}$$

where v_{wind} is the wind speed.

Fig. 3 shows the power characteristics at rated wind speed. When the grid frequency is nominal, i.e., $\Delta\omega_{ss} = 0$, the steady-state power satisfies $p_{ss} = P_{mppt}$, and the WTG operates at point A. Following a frequency drop, the output power p temporarily increases due to the frequency-support characteristics of the GFM control, which reduces the rotor speed. If the frequency returns to its nominal after the disturbance, the WTG will recover to point A after the transient dynamics, and no issue will occur. However, if the droop characteristics result in $\Delta\omega_{ss} < 0$ before the activation of secondary frequency regulation, the p_{ss} curve will shift upward, as shown in Fig. 3, driving the operating point from A to B after the disturbance. The rotor speed then settles at a lower value, causing the WTG output power to decrease, therefore deteriorating the frequency decline instead of supporting it. As shown in Fig. 3, when the wind speed changes, e.g., decreases, the curve of P_w shifts downward. Since the p_{ss} curves remain unchanged, the corresponding operating points will move to A′ and B′. Obviously, the analysis on points A and B holds for A′ and B′. Therefore, although the above analysis is presented using the rated wind speed as an example, the conclusions can be directly applied to other wind speed conditions. Moreover, regardless of the values of D_p and H, the shifting of the p_{ss} curve will always occur. The same generalities apply to all the following sections and figures.

979-8-3315-8138-1

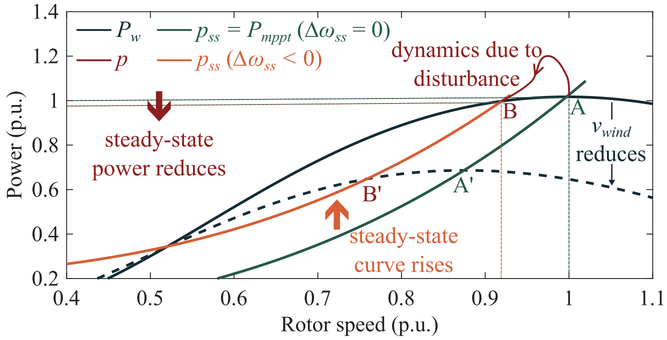

Fig. 3. Power characteristics of GFM-PMSG-WTG at rated wind speed when grid frequency is decreased after primary frequency regulation $\Delta\omega_{ss} < 0$.

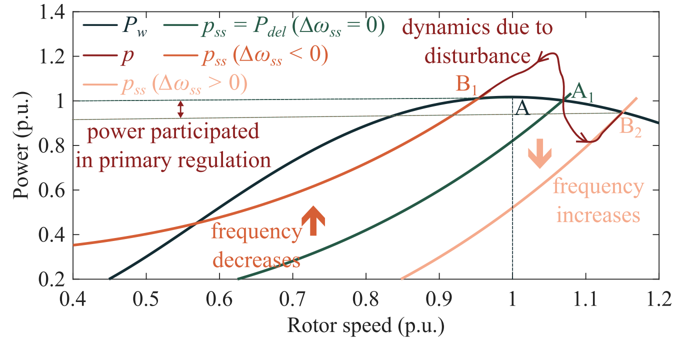

Fig. 4. Power characteristics of GFM-PMSG-WTG at rated wind speed with $d = 10$.

2) Characteristics with Typical Deloaded Operation: To enhance the capability of WTGs in primary frequency regulation, the GFM-WTG can operate in a deloaded mode instead of the MPPT mode. A typical approach is to set P_{st} to a deloaded reference P_{del}, defined as

$$P_{st} = P_{del} \coloneqq (1 - d\%)P_{mppt} \tag{8}$$

where d is the deloading level [9]. Nevertheless, the exact relationship between d and the primary frequency regulation performance remains unclear, and using (8) may still result in undesirable characteristics.

Fig. 4 shows the power characteristics with a deloading level of $d = 10$. The applied deloading shifts the P_{del} curve below P_{mppt}. It is noticed that the operating point at the rated frequency shifts from point A to A_1. When a small frequency decrease occurs, the operating point moves from A_1 to A based on the droop characteristics, releasing the deloaded power to support the grid. Nevertheless, two issues may remain. First, during a large frequency decrease, the operating point may cross A into a low-speed region, such as B_1 in Fig. 4, which is similar to the issue in Fig. 3. Second, as shown in Fig. 4, if the grid frequency increases, the steady-state curve p_{ss} goes downward, causing the operating point of the WTG to settle at point B_2 after the transient response. In this case, the output power decreases to suppress the frequency rise. Therefore, the actual power range contributing to primary frequency regulation is between points B_2 and A. However, the magnitude of this range and whether it aligns with the allowable limits remain uncertain.

III. Proposed Cooperative Strategy

This paper proposes a cooperative strategy between the GFM-WTGs and primary frequency regulation based on predefined performance specifications. Specifically, the proposed method aims to achieve the following objectives:

1) Given an allowable maximum frequency deviation for primary regulation, $\pm\Delta\omega_{ssmax}$, within which the secondary frequency regulation may not be activated in time, the droop characteristics should be well-behaved and prevent the operating point from crossing point A, therefore avoiding the negative effects illustrated in Fig. 3(b) and Fig. 4.
2) Given a maximum power reserve of $p_{sv}\%$, the actual power range participating in primary frequency regulation due to the droop characteristics should match it.

A. Frequency deviation cooperation

According to (1) and (2), the steady-state output power under primary frequency regulation can be expressed as

$$p_{ss} = P_{st} - D_p\Delta\omega_{ss}. \tag{9}$$

To satisfy the frequency deviation requirement in objective 1), the output of the WTG should increase as the grid frequency decreases. When the frequency deviation reaches its allowable maximum value, the WTG should also deliver its maximum power output to provide the greatest frequency support. Thus, the steady-state characteristics in (9) are designed to pass through the point ($\Delta\omega_{ss}$, p_{ss}) = ($-\Delta\omega_{ssmax}$, P_{mppt}), i.e.,

$$P_{mppt} = P_{st} + D_p\Delta\omega_{ssmax}. \tag{10}$$

As a result, the function in (3) is designed to

$$P_{st} = P_{mppt} - D_p\Delta\omega_{ssmax} \tag{11}$$

Fig. 5 shows the new power characteristics at the rated wind speed. At the rated grid frequency, the WTG operates in a deloaded mode at point C. Unlike conventional deloaded operation, the deloading level is automatically determined by (11) and the wind power characteristics given in (7) rather than being predefined. As the grid frequency decreases, the WTG increases its output power, and the operating point moves from C to B. When the frequency deviation reaches its maximum value, the operating point moves to the MPPT point A. Within the frequency regulation range of [$-\Delta\omega_{ssmax}$, 0], the WTG effectively participates in the primary frequency regulation and the operating point is effectively prevented from crossing point A, therefore avoiding the adverse issue observed in conventional schemes.

B. Power Reserve Cooperation

In addition to responding to frequency decreases, the GFM-WTG should also reduce its output when the grid frequency exceeds the rated value. However, the power reduction should be limited to avoid unnecessary curtailment of wind energy. Therefore, a maximum power reserve $p_{sv}\%$ can be predefined.

979-8-3315-8138-1

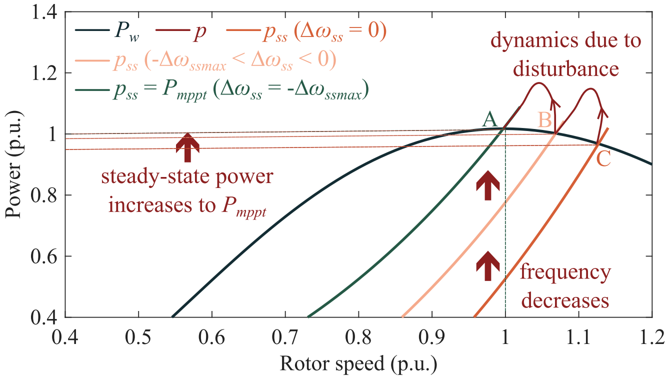

Fig. 5. Power characteristics of GFM-PMSG-WTG at rated wind speed with proposed frequency deviation cooperation strategy.

In this paper, $p_{sv} = 10$ is used. Accordingly, when the WTG output decreases to 90%, it should not be further reduced. Other more expensive generation sources can go on to decrease their outputs.

Fig. 6 shows the characteristics of the power coefficient C_p [13]. The power coefficient of 0.9 p.u. is used to determine the tip speed ratio corresponding to the reserved power, which is denoted as λ_{prim}. Accordingly, the lowest power considering primary frequency regulation, P_{lim}, is defined as

$$P_{lim} := \frac{1}{2}\rho\pi R^5 C_{prim}(\lambda_{prim},\ \beta)\frac{\omega_m^3}{\lambda_{prim}^3}. \tag{12}$$

To achieve coordinated power reserve participation, the lower limit of the steady-state characteristics in (9) is designed to pass through the point ($\Delta\omega_{ss}$, p_{ss}) = ($\Delta\omega_{ss}$, P_{lim}), i.e.,

$$P_{lim} = P_{st} - D_p\Delta\omega_{ss}. \tag{13}$$

Accordingly, the lower boundary of the function in (3) should be expressed as

$$P_{st} = P_{lim} + D_p\Delta\omega_{ss}. \tag{14}$$

Fig. 7 shows the power characteristics at the rated wind speed with power reserve cooperation. The WTG operates at point A at the rated frequency as illustrated in (11). As the grid frequency increases, the WTG decreases its output power, and the operating point moves from A to B. When the frequency further increases, the operating point may move to point C_1, leading the output beyond the maximum 10% power reserve. In this context, by applying (14), the operating point will converge to the limit point of C_2 instead of C_1 after the transient response.

By combining (11) and (14), the function in (3) is proposed as

$$P_{st}(\omega_m) = \max\{P_{mppt} - D_p\Delta\omega_{ssmax},\ P_{lim} + \frac{D_p}{T_{prim}s+1}\Delta\omega\} \tag{15}$$

where T_{prim} is a constant time for deriving $\Delta\omega_{ss}$ and $\Delta\omega$ can be obtained from the GFM control in Fig. 2 and (2). It should be noted that the proposed strategy is also based on the deloading

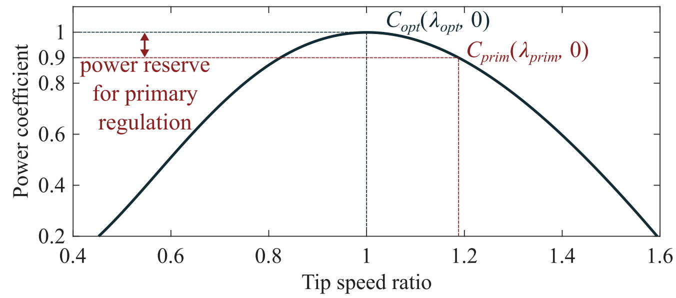

Fig. 6. Characteristics of power coefficient C_p.

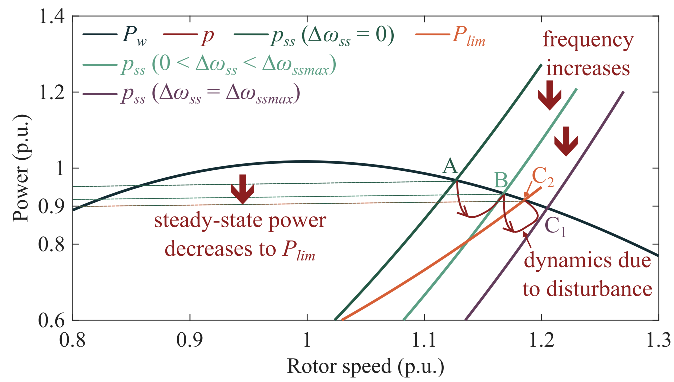

Fig. 7. Power characteristics of GFM-PMSG-WTG at rated wind speed with proposed cooperation strategy.

scheme and the methodology for analyzing the operating point movement is similar to that used for conventional strategies. Nevertheless, the specific implementation of the proposed design is fundamentally different.

IV. Case Studies

A 5 MW/690 V PMSG-WTG is used to evaluate the performance of the proposed scheme. The maximum frequency deviation and power reserve are set to $\pm\Delta\omega_{ssmax} = \pm 0.5$ Hz (± 0.01 p.u.) and $p_{sv}\% = 10\%$, respectively. The droop coefficient of the GFM control is chosen as 50 p.u. The proposed strategy is compared to the conventional MPPT control and deloaded control schemes with 10% and 20% deloading levels.

A. Grid Frequency Decrease

Fig. 8 shows the simulation results, where the grid frequency first decreases to 0.997 p.u. and subsequently to 0.9925 p.u. Although the MPPT control provides transient power support, its steady-state output decreases instead of increasing, therefore failing to sustain frequency regulation. The deloaded control [9] with a 10% deloading level mitigates the steady-state power reduction to some extent but cannot eliminate it completely. When the deloading level is increased to 20%, the WTG is able to increase its output when the frequency decreases to 0.997 p.u. However, as the grid frequency further drops to 0.9925 p.u., the output begins to decline again. This indicates that the operating point has crossed the MPPT

979-8-3315-8138-1

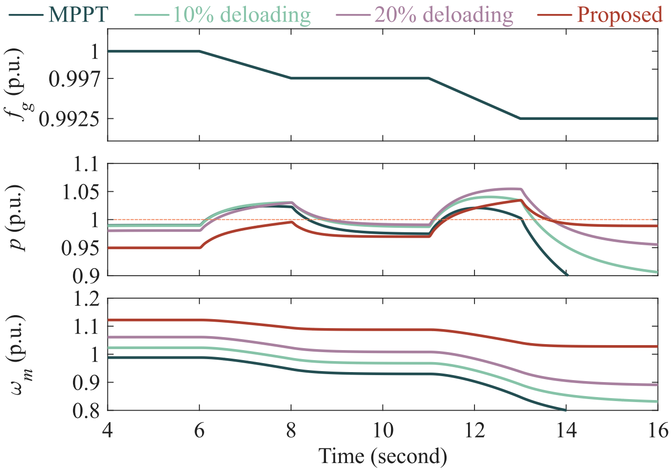

Fig. 8. Simulation results when grid frequency decreases.

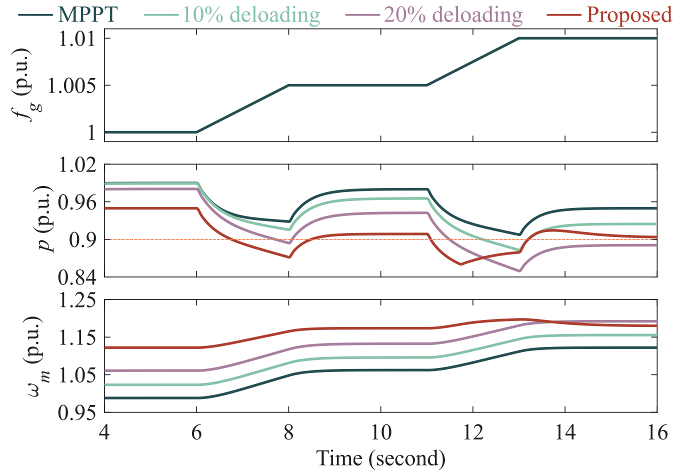

Fig. 9. Simulation results when grid frequency increases.

point, as seen from the reduced rotor speed, which ultimately deteriorates the frequency regulation performance. In contrast, the proposed strategy effectively supports the grid frequency by increasing the output power in both the transient and steady-state periods.

B. Grid Frequency Increase

Fig. 9 shows the simulation results, where the grid frequency first rises to 1.005 p.u. and subsequently to the maximum value of 1.01 p.u. As observed, under both MPPT control and the 10% deloaded control [9], there remains unused regulation capability even when the frequency reaches its upper limit, which means that the allowable power reserve for primary regulation has not been fully used. In contrast, the output of the 20% deloaded mode eventually drops below 0.9 p.u., exceeding the predefined power reserve limit. With the proposed strategy, the WTG appropriately reduces its output to stabilize the grid frequency when the limit has not been reached. Once the maximum allowable reserve is met, the output will converge to the limit, therefore ensuring full utilization of the power reserve without exceeding it.

V. Conclusion

This paper proposes a cooperative strategy between GFM-WTGs and primary frequency regulation. Based on the predefined specifications for the allowable maximum frequency deviation and power reserve, the WTG can emulate droop characteristics similar to those of conventional SGs within the specified limits. Specifically, as the grid frequency decreases toward its lower limit, the WTG increases its output up to the maximum power without further crossing the maximum power point. As the frequency rises toward the upper limit, the WTG decreases its output to the predefined power reserve without exceeding it.

References

[1] F. Blaabjerg, M. Chen, and L. Huang, “Power electronics in wind generation systems,” *Nat. Rev. Electr. Eng.*, vol. 1, pp. 234–250, Apr. 2024.

[2] A. González-Cajigas, E. J. Bueno, J. Roldán-Pérez, R. Martín-López, and E. Sáiz-Marín, “Control choices to allow the parallel operation of grid-forming Type-III wind turbines,” *IEEE Trans. Power Electron.*, vol. 38, no. 12, pp. 15 353–15 364, Dec. 2023.

[3] M. Kang, K. Kim, E. Muljadi, J.-W. Park, and Y. C. Kang, “Frequency control support of a doubly-fed induction generator based on the torque limit,” *IEEE Trans. Power Syst.*, vol. 31, no. 6, pp. 4575–4583, 2016.

[4] D. Yang, J. Kim, Y. C. Kang, E. Muljadi, N. Zhang, J. Hong, S.-H. Song, and T. Zheng, “Temporary frequency support of a DFIG for high wind power penetration,” *IEEE Trans. Power Syst.*, vol. 33, no. 3, pp. 3428–3437, May 2018.

[5] Y. Zhou, D. Zhu, X. Zou, C. He, J. Hu, and Y. Kang, “Adaptive temporary frequency support for DFIG-based wind turbines,” *IEEE Trans. Energy Convers.*, vol. 38, no. 3, pp. 1937–1949, Sep. 2023.

[6] A. Bonfiglio, M. Invernizzi, A. Labella, and R. Procopio, “Design and implementation of a variable synthetic inertia controller for wind turbine generators,” *IEEE Trans. Power Syst.*, vol. 34, no. 1, pp. 754–764, Jan. 2019.

[7] Y. Tang, P. Yang, Y. Yang, Z. Zhao, and L. L. Lai, “Fuzzy adaptive frequency support control strategy for wind turbines with improved rotor speed recovery,” *IEEE Trans. Sustain. Energy*, vol. 15, no. 2, pp. 1351–1364, Apr. 2024.

[8] T. Zhao, H. Liu, N. Wang, J. Su, Z. Luo, and S. Ma, “An active power control of DFIG-based wind turbine generators for frequency regulation with expected dynamic performance,” *Appl. Energy*, vol. 391, 2025.

[9] W. Bao, L. Ding, Y. C. Kang, and L. Sun, “Closed-loop synthetic inertia control for wind turbine generators in association with slightly over-speeded deloading operation,” *IEEE Trans. Power Syst.*, vol. 38, no. 6, pp. 5022–5032, Nov. 2023.

[10] T. Zhao, H. Liu, J. Su, N. Wang, and Z. Luo, “Coordinated control for distributed energy resources in islanded microgrids with improved frequency regulation capability,” *Renew. Energy*, vol. 244, May 2025.

[11] M. Chen, D. Zhou, A. Tayyebi, E. Prieto-Araujo, F. Dörfler, and F. Blaabjerg, “On power control of grid-forming converters: Modeling, controllability, and full-state feedback design,” *IEEE Trans. Sustain. Energy*, vol. 15, no. 1, pp. 68–80, Jan. 2024.

[12] M. Chen, D. Zhou, and F. Blaabjerg, “Multivariable grid-forming converters with direct states control,” *IEEE Trans. Ind. Appl.*, vol. 59, no. 4, pp. 4334–4341, Jul./Aug. 2023.

[13] X. Lyu and D. Groß, “Grid forming fast frequency response for PMSG-based wind turbines,” *IEEE Trans. Sustain. Energy*, vol. 15, no. 1, pp. 23–38, Jan. 2024.

[14] X. Yuan, Z. Du, Y. Li, Y. Xu, J. Li, D. Yu, H. Peng, and Z. Xu, “Two-stage coordinated control of Type-4 wind turbine with grid-forming ability for active damping support,” *IEEE Trans. Energy Convers.*, vol. 39, no. 2, pp. 817–830, Jun. 2024.

[15] A. González-Cajigas, E. J. Bueno, and J. Roldán-Pérez, “Compliance of grid-forming requirements of grid codes with a Type III wind turbine controlled as a virtual synchronous machine,” *IEEE Transactions on Energy Conversion*, vol. 39, no. 4, pp. 2244–2257, Dec. 2024.

979-8-3315-8138-1